Supporting Information

Biomass-Derived Two-dimensional N,O-doped carbon Embed binary-metal nanoparticles Enable Dendrite-Free Potassium-Metal Anodes

Qing Shen[a], Yibo He[a], and Junjie Wang[a]*

[a]State Key Laboratory of Solidification Processing, School of Materials Science and Engineering, Northwestern Polytechnical University, Xi'an, Shaanxi 710072, People's Republic of China.

* Corresponding author.

E-mail address: wang.junjie@nwpu.

Experimental section:

Preparation of composite anodes

NiCo@NOGC was synthesized along following procedures. Firstly, 2 g dried leaves and 30 ml deionized water were added into a 50 mL Teflon-lined autoclave and kept at 200 °C for 8 hours. The precipitate was collected by centrifugation, rinsed with deionized water and ethanol, and dried at 70 °C for 12 h to obtain biomass carbon materials. Next, 0.1 g cobaltous nitrate ($Co(NO_3)_2 \cdot 6H_2O$), 0.1 g nickel nitrate ($Ni(NO_3)_2 \cdot 6H_2O$), and 0.3 g biomass carbon materials were vigorously stirred for 10 minutes. After the raw materials were fully mixed, the obtained blackening solution was transferred to a 50 ml Teflon-lined autoclave and heated to 200 ℃ for 8 h. After natural cooling to room temperature, the dark brown precipitate was collected by centrifugation and rinsed with deionized water and ethanol, and then dried under vacuum at 70 °C for 12 h. The collected dark powder was then annealed under an argon atmosphere at 600 °C for 6 h with a heating rate of 3 °C min^{-1}. NiFe@NOGC (CoFe@NOGC) can be synthesized by the same method as NiCo@NOGC using $Ni(NO_3)_2 \cdot 6H_2O$, $Fe(NO_3)_3 \cdot 9H_2O$, ($Co(NO_3)_2 \cdot 6H_2O$ and $Fe(NO_3)_3 \cdot 9H_2O$). All reagents used in this study were purchased from Sigma-Aldrich without further purification.

Material characterization

The morphology and microstructures of synthesized samples were investigated by Scanning Electron Microscope（SEM, ZEISS sigma 300), Transmission electron microscopy (TEM, FEI Talos F200X), X-Ray Diffraction (XRD, Bruker D8 Advance), X-ray Photoelectron Spectroscopy (XPS, Thermo Scientific ESCALAB 250Xi),

Raman spectra (laser wavelength of 512 nm), and Fourier Transform Interferometric Radiometer (FTIR, Bruker INVENIO S). The specific surface areas of all samples were calculated using the multi-point Brunel–EmmettTeller (Tellwe,BET) method.

Electrochemical measurements

All batteries were assembled with standard 2032-type coin cells in an argon-filled glove box (MIKROUNA, O_2, and H_2O<0.01 ppm). The working electrodes were prepared by casting the slurry mixture of active materials (NiCo@NOGC), carbon black, and poly vinylidene fluoride (PVDF) at a mass ratio of 7:2:1 on a Cu foil. The coated foil was dried under vacuum at 60 °C for 12 h and then cut into discs with a diameter of 12 mm. The area mass load of the active substance is about 0.9 to 1.1 mg cm^{-2}. NiFe@NOGC and CoFe@NOGC coated electrodes were fabricated through a similar process. The glass microfiber separators (Whatman, CF/F) were used in all kinds of batteries in this work. 1 M potassium bis(fuorosulfony)imide (KFSI) in ethylene carbonate (EC) and Diethyl carbonate (DEC) (1:1, in volume) were employed here as electrolytes (80 μL) for the tests of asymmetrical and symmetrical cells. The bare K foils were served as the counter and reference electrodes. For galvanostatic analysis, asymmetric cells first underwent 5 "formation cycles" from 0.01 to 1 V at 50 μA cm^{-2}, which cleaned the surfaces from any residual impurities and stabilized the SEI layer without plating K metal. To test the Coulombic efficiency, a fixed amount of K was plated on the anode and stripped up to 1 V during the plating/stripping cycle. The electrodes used in the symmetric cells were pre-deposited with a K area capacity of 4 mAh cm^{-2} (K-NiCo@NOGC). A bare K metal electrode and K-NiCo@NOGC mesh electrodes were

used as the anode, and Prussian blue (PB) electrode was used as the cathode for assembling K metal full batteries. PB prepared according to previous literature [1]. To test the K-NiCo@NOGC||PB full cells, the cathode was prepared by casting the slurry mixture of PB, carbon black and polyvinylidene fluoride with a mass ratio of 6:3:1 on Al foil, which was dried in a vacuum oven at 60 ℃ for 12 h . The areal mass loading of PB cathode is about 3.0 mg cm^{-2}. The electrolyte employed in full cells is 0.8 M KPF_6 in ethylene carbonate (EC)/diethyl carbonate (DEC) (1:1 volume ratio) in a volume of 40 μL. The full batteries were tested in the voltage range of 1.5–3.8 V. Electrochemical performances of all batteries were tested by using a Neware test system. EIS measurements were performed using a CHI 660 electrochemical workstation in the frequency range of 0.1-100 KHz. To observe the morphology of K on the current collector, the cell was first disassembled in a glove box filled with ar. The plated or stripped anode was then rinsed with diethyl carbonate (DEC) to remove residual electrolyte and salt, then dried in the glove box at room temperature and characterized.

Computational details

Vienna *Ab-initio* Simulation Package (VASP) [2]was used for all density functional theory (DFT)-based calculations of this work. The projector augmented plane-wave (PAW) [3]method and the Perdew–Burke–Ernzerhof (PBE)[4] functional within generalized gradient approximation (GGA) were employed to calculate the exchange-correlation interaction energy. Thereby, electrons in orbits of 8*d*1*s* for Co and Ni, 2*s*2*p*

for C, 2*s*4*p* for O, 2*s*3*p* for N, 3*s*3*p* for K, and 1*s* for H were deemed as valence electrons according to the pseudopotential method. For the structural optimizations of alloy NiCo (111) and graphene, a 3× 3 × 1 supercell and a 3 × 4 × 1 supercell with a 20 Å vacuum were constructed, respectively. And we optimized slab models consisting of graphene monolayer adsorbed on the (111) surface of the face-centered cubic (FCC) NiCo crystals in our simulations. The plane-wave cutoff energy, convergence criterion of self-consistent iterations, and convergence force on each atom were set to be 520 eV, 1×10^{-6} eV, and 0.04 eV/Å, respectively. The Monkhorst-Pack *k*-point meshes were sampled using a 5 × 5 × 1 for the relaxation and total energy calculations of slab models. The Monkhorst-Pack k-point mesh of 5 × 5 × 1 was used after a convergence test (Fig S1). And adsorption energies (E_b) of K on different graphene surfaces were calculated using the following equation:

$$E_b = E_{k@surf} - E_{surf} - E_k \quad (1)$$

where $E_{k@surf}$, E_{surf} and E_k are the calculated energies of K@surface, the bare surface and a K atom in the most stable K metal phase, respectively.

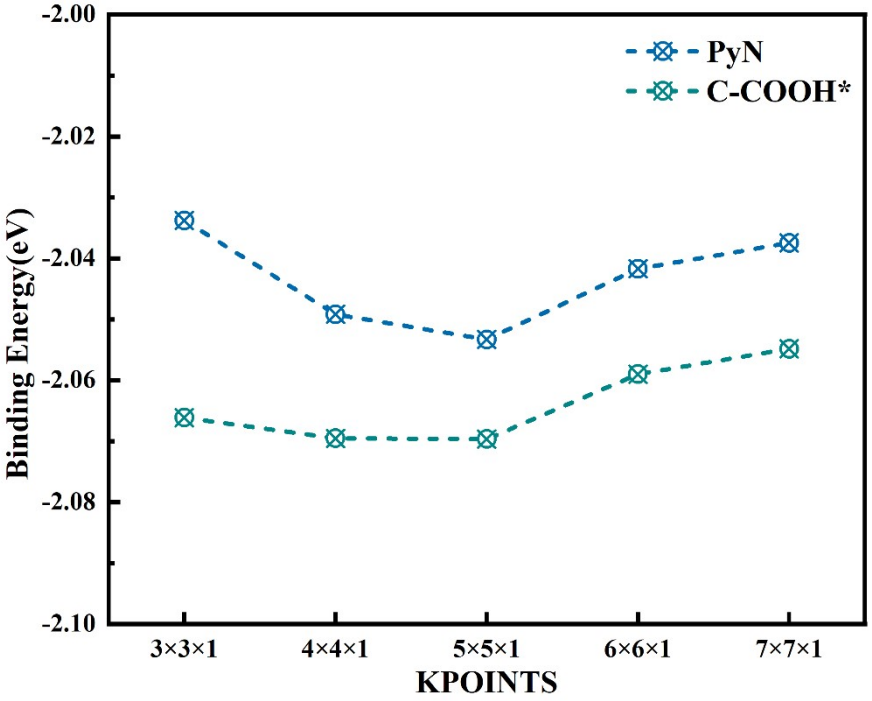

Fig S1:. The calculated binding energy of graphene with different groups as a function of KPOINTS.

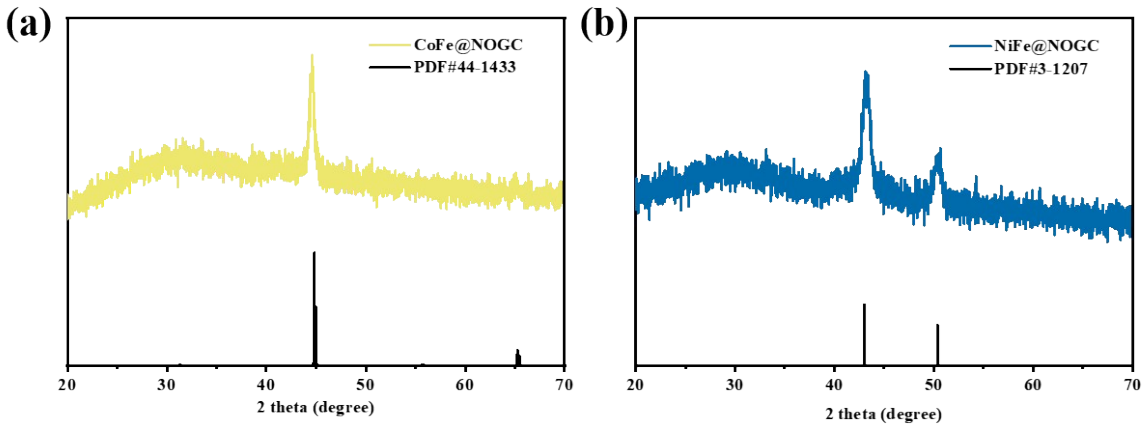

Fig S2: (a) XRD patterns of NiFe@NOGC and (b) CoFe@NOGC.

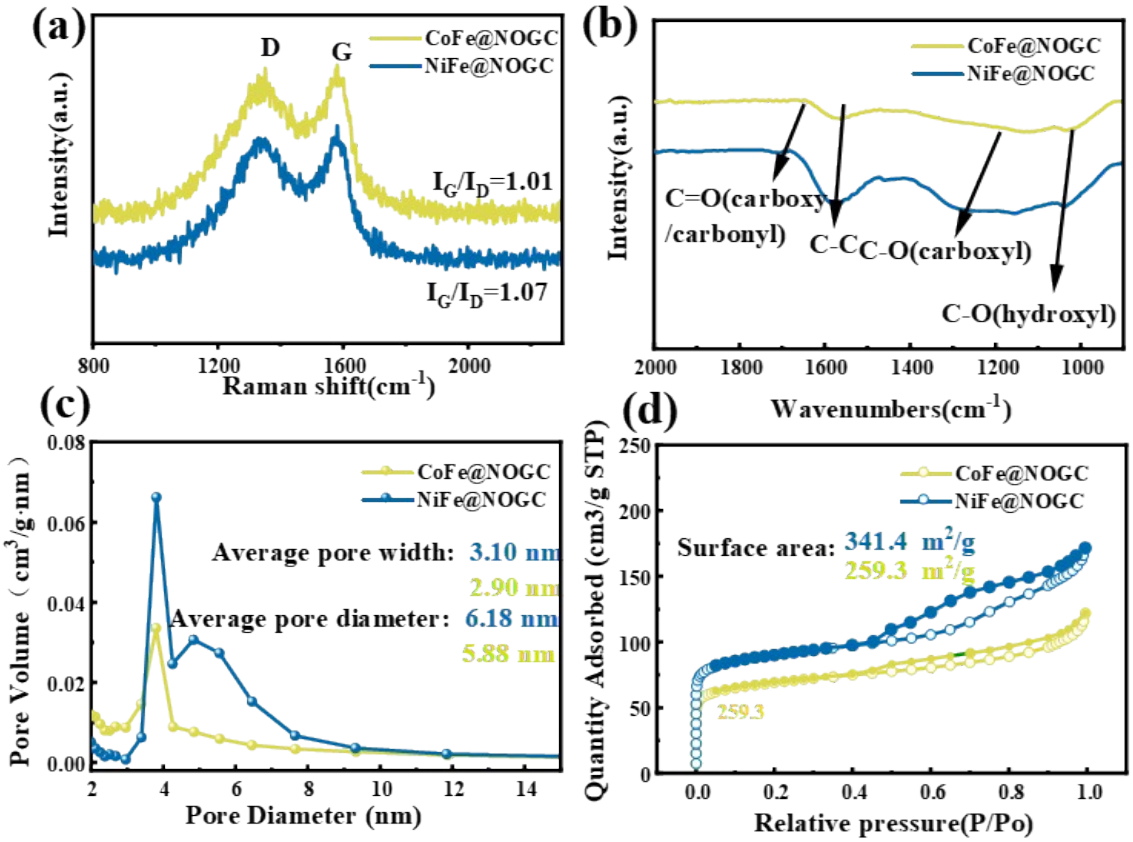

Fig S3: Structure characterization of synthesized NiFe@NOGC and CoFe@NOGC composite. (a) XRD patterns; (b) FTIR spectra; (c)pore size distribution and (d) Nitrogen adsorption-desorption isotherms curve.

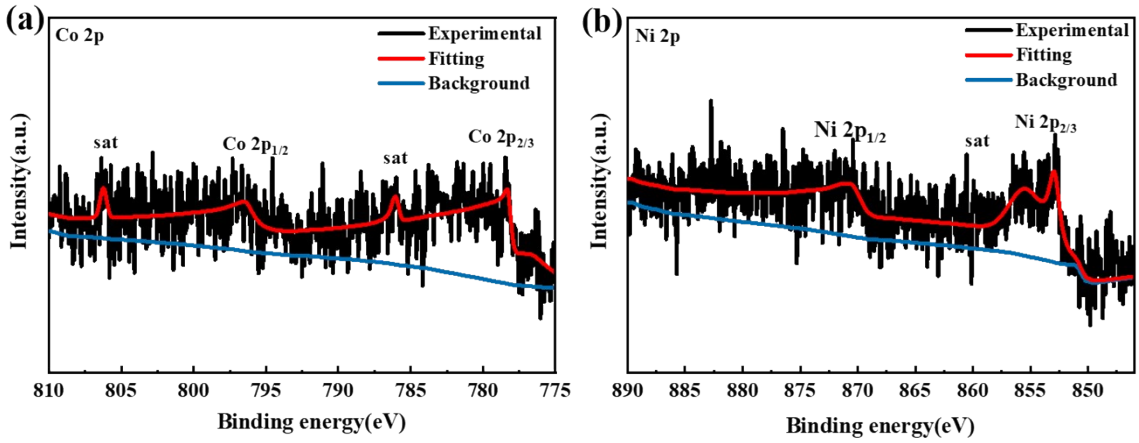

Fig S4: (a) High-resolution XPS spectra of NiCo@NOGC Co 2p and (b) Ni 2p.

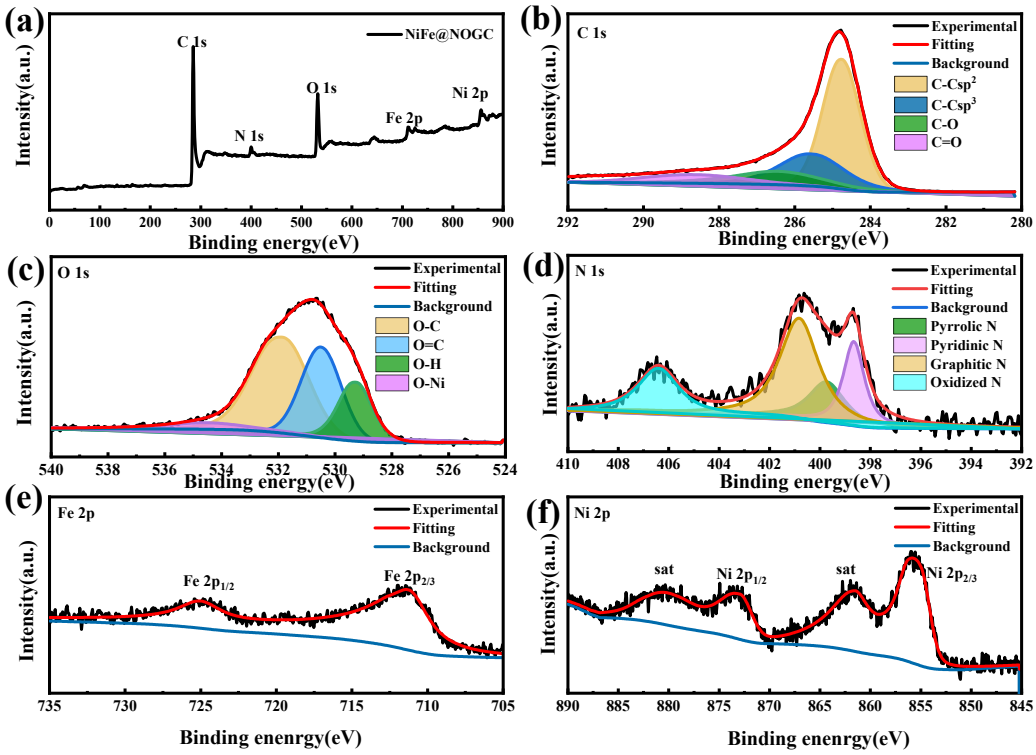

Fig S5: XPS spectra of NiFe@NOGC nanocomposite: (a) survey spectrum, (b) S2p spectrum, (c) C 1s spectrum, (d) N 1s spectrum, (e) Fe 2p spectrum, (e) Ni 2pspectrum.

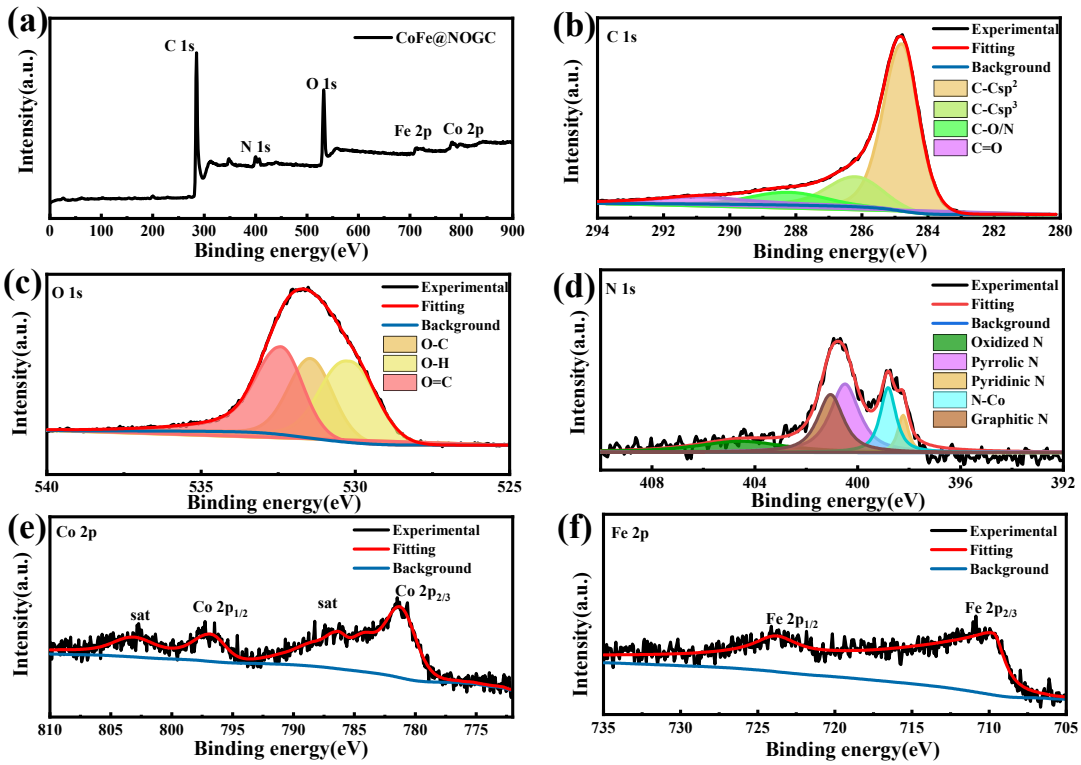

Fig S6: XPS spectra of CoFe@NOGC nanocomposite: (a) survey spectrum, (b) S2p spectrum, (c) C 1s spectrum, (d) N 1s spectrum, (e) Fe 2p spectrum, (e) Ni 2pspectrum

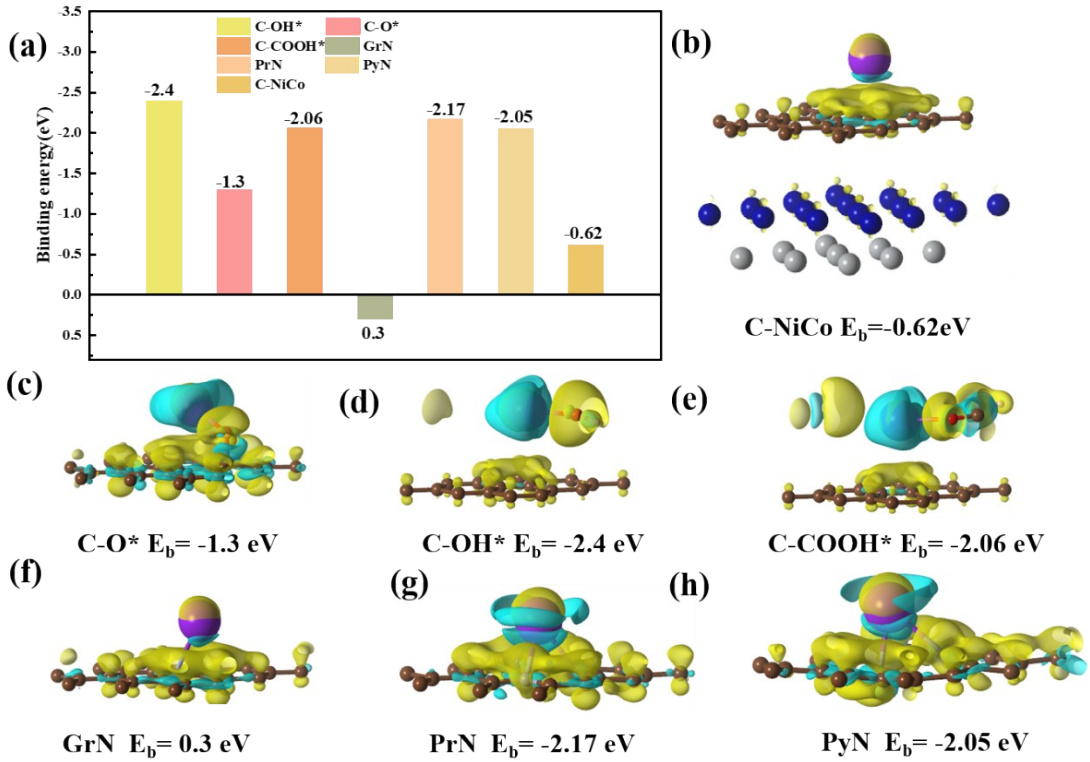

Fig. S7: (a) Binding energy of a K atom with C-NiCo and each component of graphene; (b-h) differential charge density of the interaction between a K atom with C-NiCo and different functionalized group of graphene. The yellow and cyan surfaces correspond to the charge gain and lost regions, respectively (isovalue, 0.0015). The potassium, carbon, oxygen, nitrogen, nickel and cobalt atoms are marked in purple, brown, red, light purple, grey and blue, respectively.

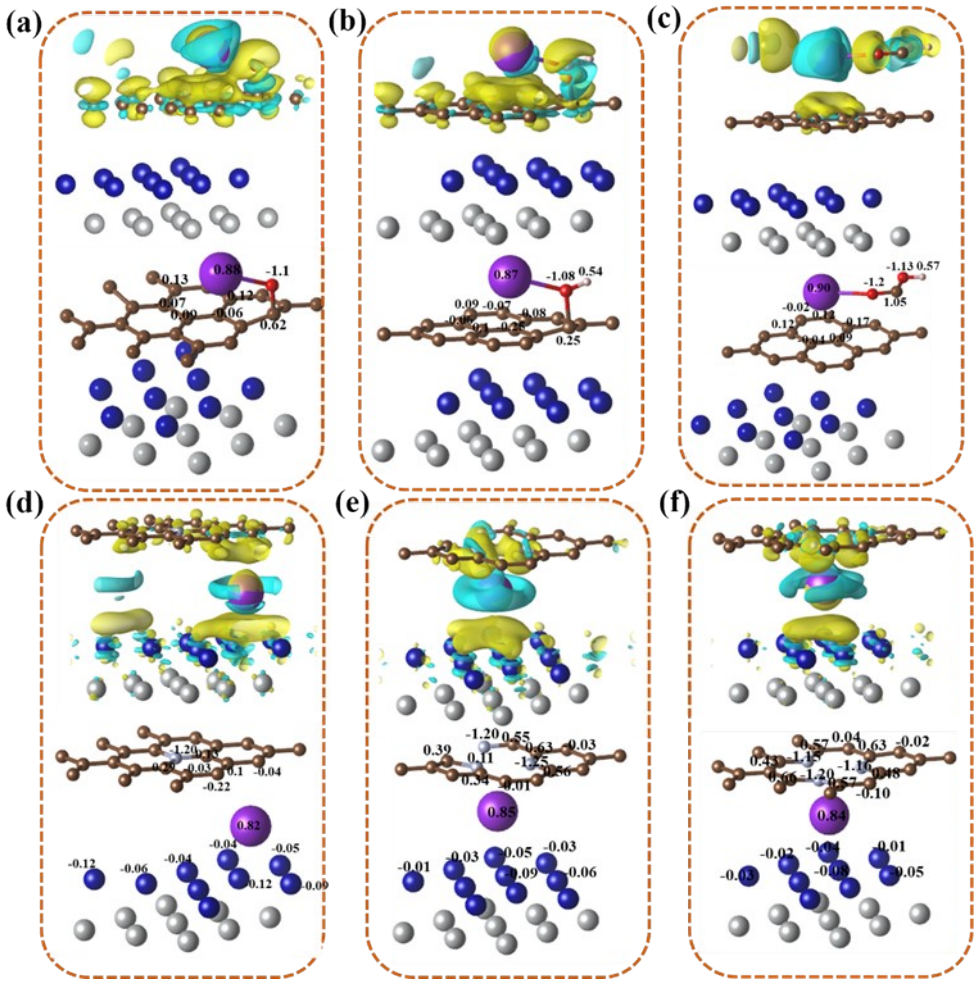

Fig S8: The calculation results of Bader charge analysis and charge density difference on the surface of NiCo@NOGC with different functional groups: a) CO-NiCo, b) OH-NiCo, c) COOH-NiCo, d) GrN-NiCo, e) PyN-NiCo, and f) PrN-NiCo group. The yellow and cyan surfaces indicate the charge gain and lost regions, respectively (isovalue, 0.0015). The potassium, carbon, oxygen, nitrogen, nickel and cobalt atoms are marked in purple, brown, red, light purple, grey and blue, respectively.

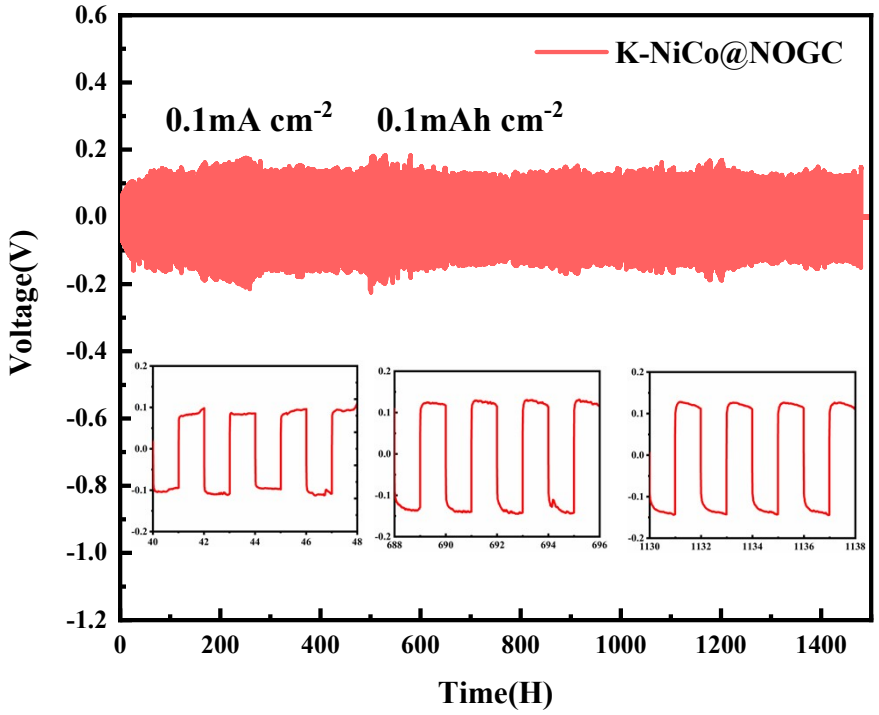

Fig S9: Voltage profiles of K plating/stripping on K-NiCo@NOGC at 0.1 mA cm^{-2} (inert Figure is the voltage profiles at the period of 40–48 h, 688–696 h, and 1130–1138 h).

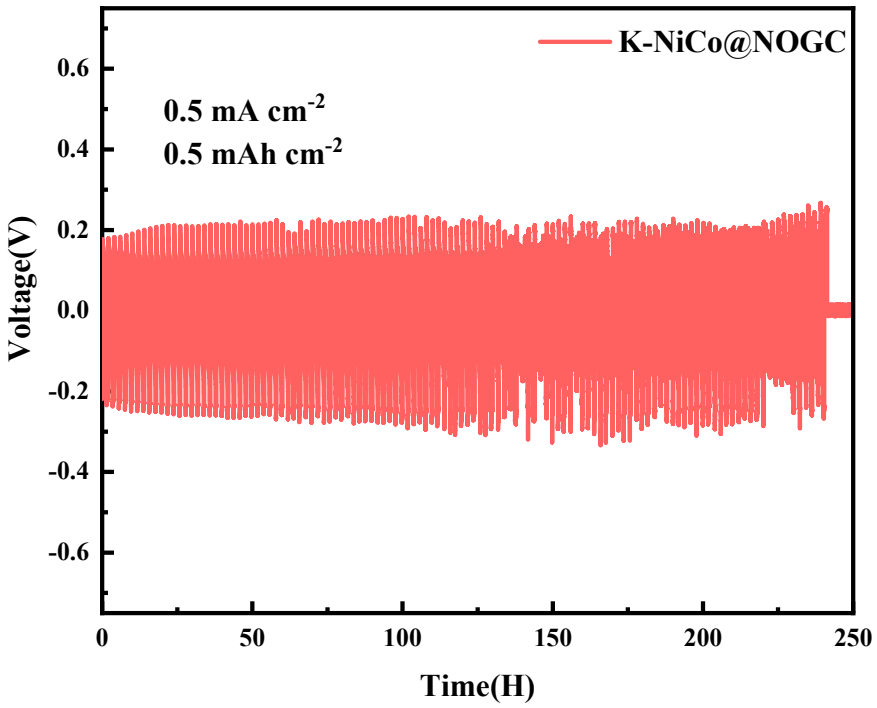

Fig S10: Voltage profiles of K plating/stripping on K-NiCo@NOGC at 0.5 mA cm^{-2}.

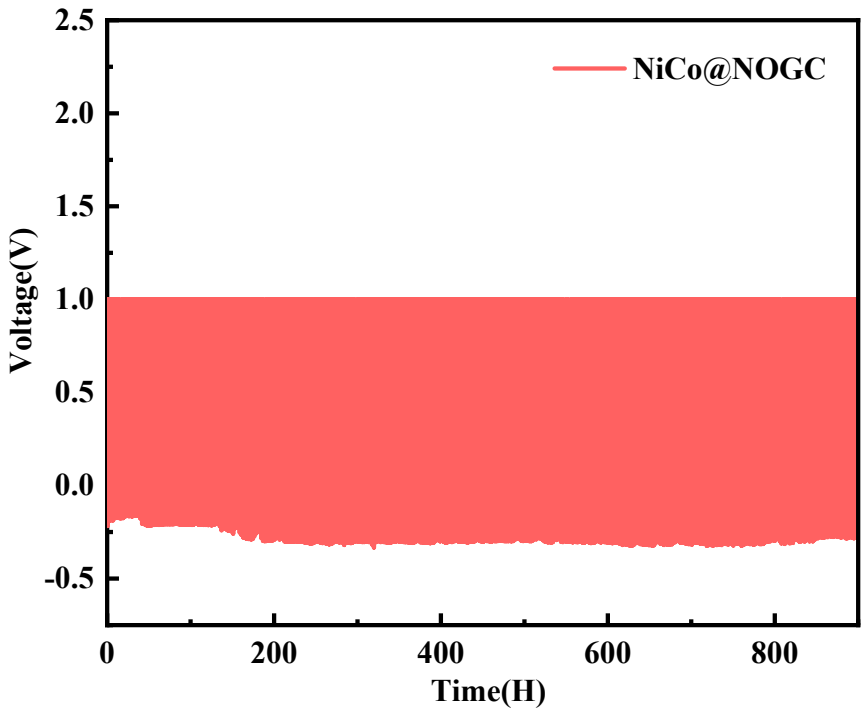

Fig S11: the curve of voltage-time of NiCo@NOGC at 0.5 mA cm^{-2} for 0.5 mAh cm^{-2}.

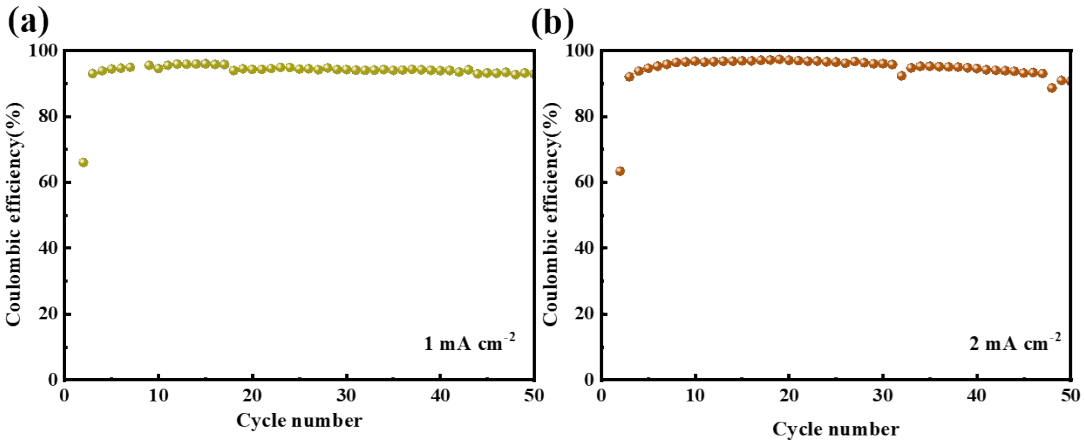

Fig S12: (a) Coulombic efficiency of NiCo@NOGC electrode with K deposition amount of 0.5 mAh cm^{-2} at 1 mA cm^{-2} and (b) 2 mA cm^{-2}.

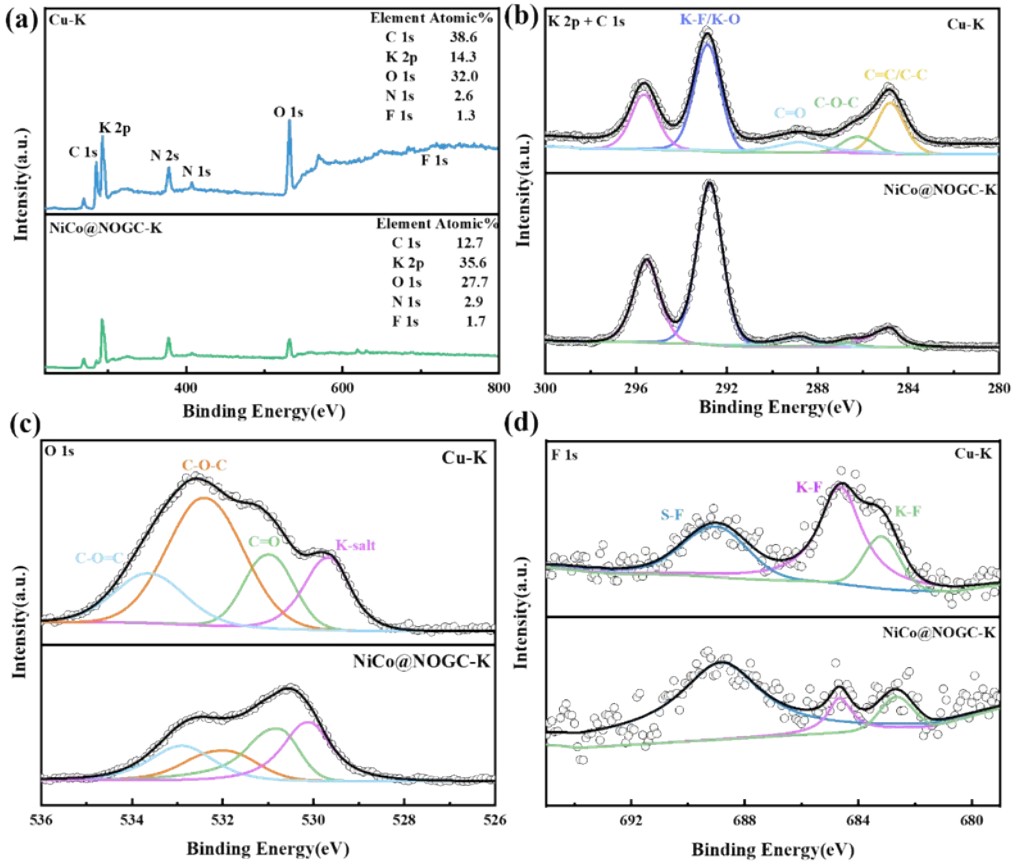

Fig S13: XPS analysis of the SEI on Cu-K and NiCo@NOGC-K after 10 plating/stripping cycles. (a) XPS survey spectra of bare K and NiCo@NOGC-K (inset lists the atoms contents of elements); (b) O 1s, (c) K 2p + C 1s, (d) F 1s XPS spectra of the cycled Cu-K and NiCo@NOGC-K.

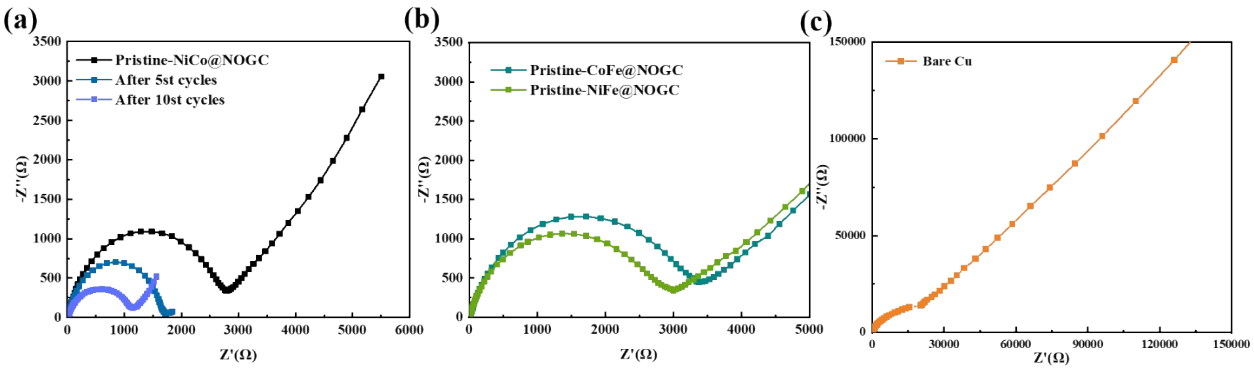

Fig S14: The Nyquist plots of (a)NiFe@NOGC, (b)CoFe@NOGC and NiCo@NOGC and (c) bare Cu copper electrodes.

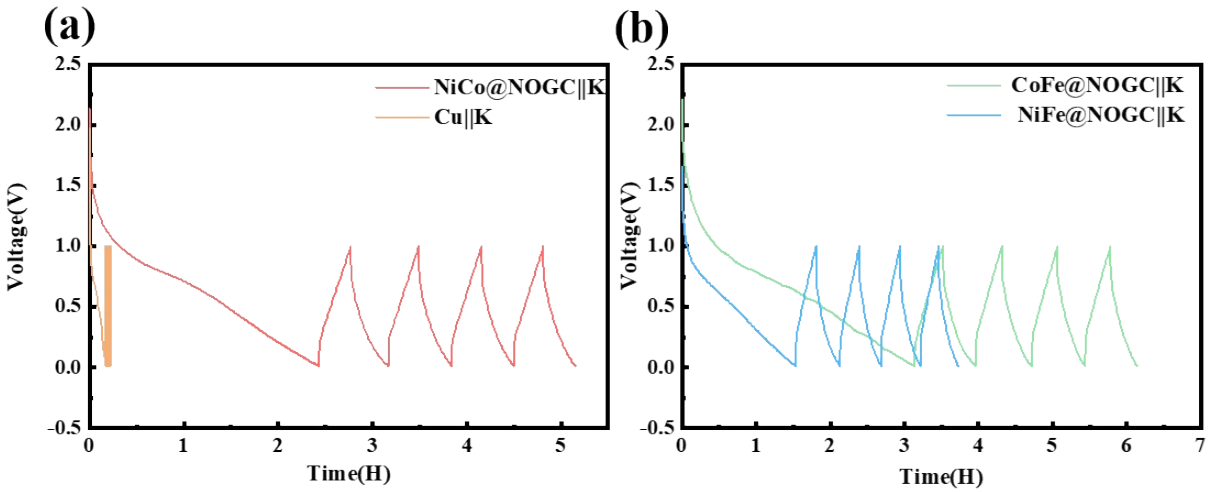

Fig S15: (a) Voltage-time profiles of five cycles of NiFe@NOGC and Cu; (b)CoFe@NOGC and NiCo@NOGC electrodes.

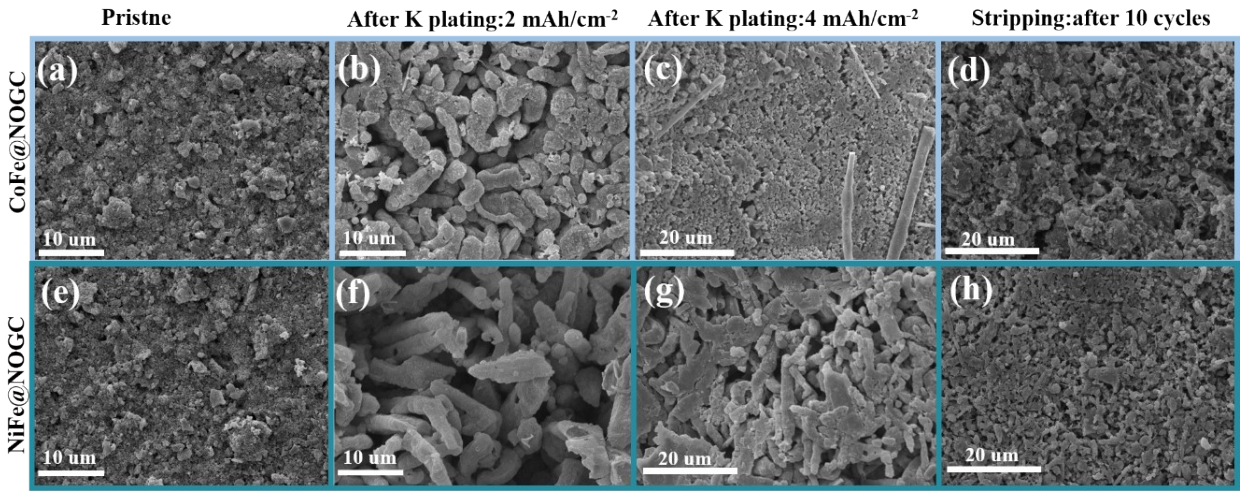

Fig S16. Morphology evolution of CoFe@NOGC and NiFe@NOGC electrode during plating/stripping. a,e) SEM image of CoFe@NOGC and NiFe@NOGC electrode without K metal; b,f) after plating 2 mAh cm^{-2}; c,g) after plating 4 mAh cm^{-2}; d h) the 10th stripping 0.5 mA cm^{-2}.

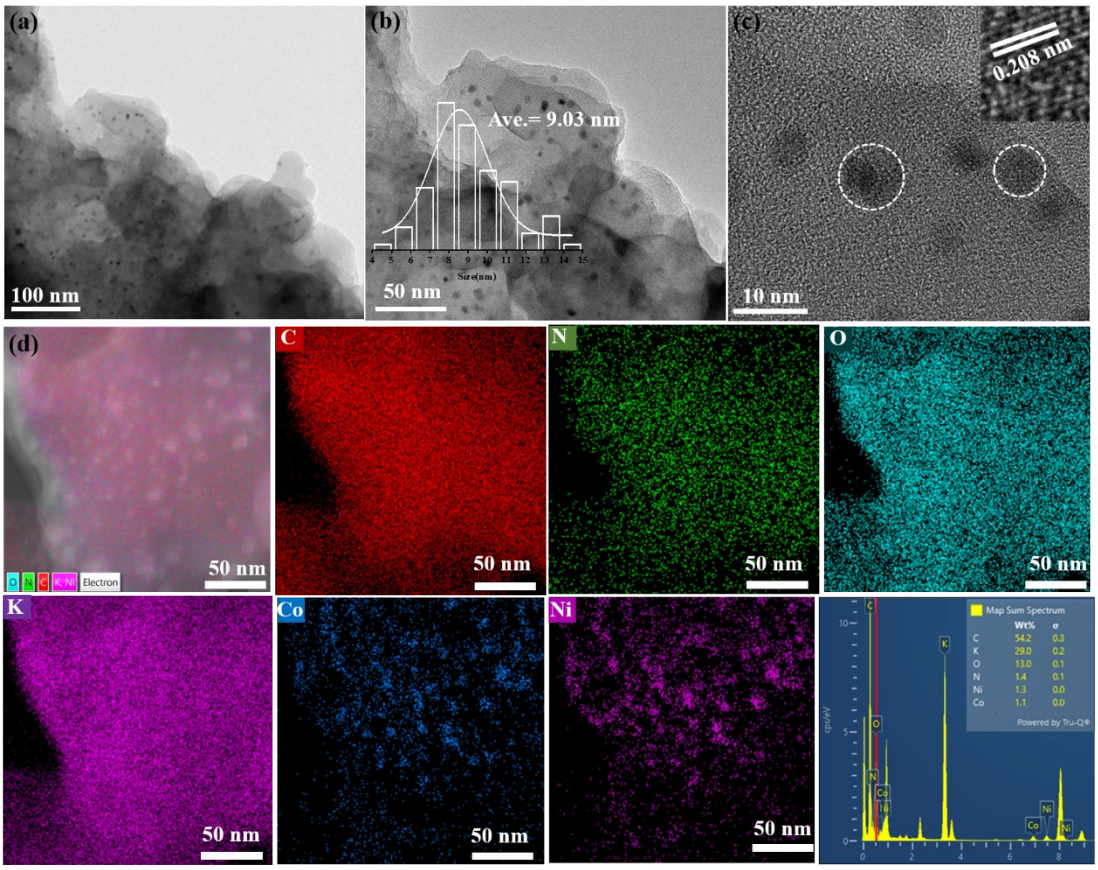

Fig S17: (a-b) TEM and (c) HRTEM images and (d) elemental mapping of NiCo@NOGC electrode after plating/stripping 10 cycles at 0.5 mA cm^{-2} for 0.5 mAh cm^{-2}.

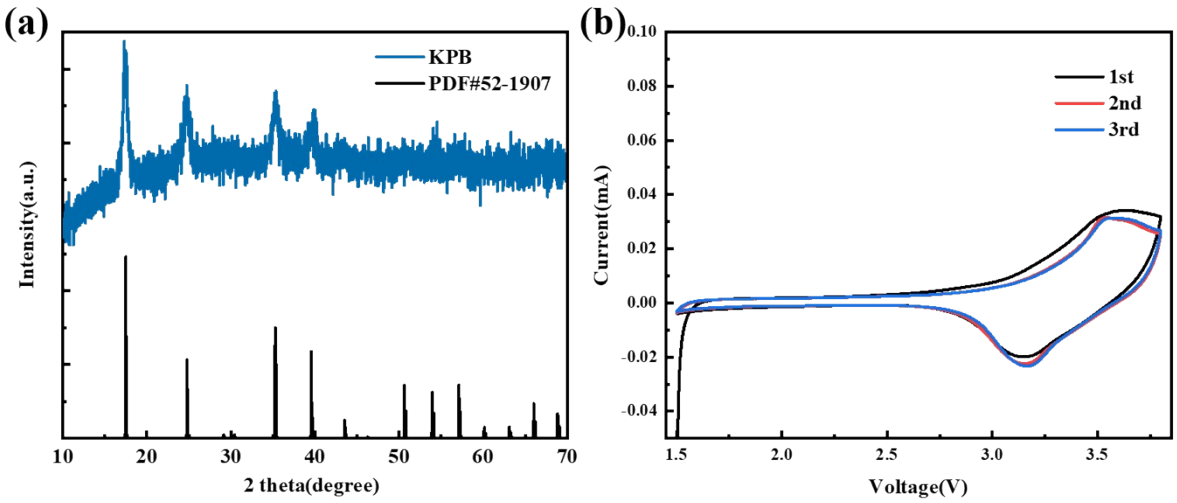

Fig S18: (a) XRD patterns and (b) curves at 0.2 mV s^{-1} of Prussian blue.

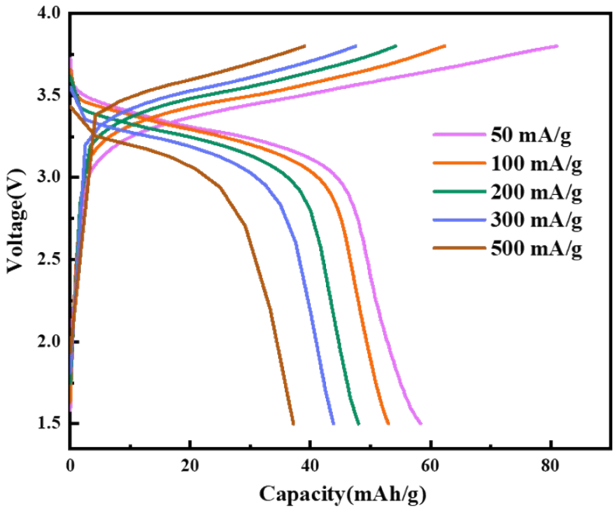

Fig S19: charge/discharge profiles of PB||pristine K.

Table S1. Element contents of NiCo@NOGC, NiFe@NOGC, and CoFe@NOGC obtained by XPS analysis.

Materials	**Element (at %)** **(wt %)**					
	C	N	O	Ni	Co	Fe
NiCo@NOGC	76.96 (71.61)	4.93 (5.7)	17.27 (19.46)	0.43 (1.44)	0.41 (1.79)	/
NiFe@NOGC	76.19 (64.77)	4.79 (5.68)	14.69 (16.89)	1.94 (6.03)	/	2.39 (6.63)
CoFe@NOGC	88.14 (78.26)	3.71 (4.66)	7.23 (9.49)	/	0.57 (2.91)	0.35 (4.68)

Table S2. The N 1s and O 1s distribution of NiCo@NOGC, NiFe@NOGC, and CoFe@NOGC obtained from the results of XPS.

Materials	Oxygen group (at %)			Nitrogen group (at %)		
	O=C	O-C	O-H	Pyridinc N	Pyrrolic N	Graphitic N
NiCo@NOGC	46.12	17.23	15.08	11.48	19.02	16.66
NiFe@NOGC	26.58	44.03	18.02	19.95	16.46	43.75
CoFe@NOGC	39.59	36.70	23.69	6.62	33.95	25.45

Table S3. The contents of NiCo@NOGC, NiFe@NOGC, and CoFe@NOGC based on ICP-OE analysis.

Materials	Element (wt %)		
	Ni	Co	Fe
NiCo@NOGC	3.69	4.28	/
NiFe@NOGC	18.15	/	9.45
CoFe@NOGC	/	11.3	15.68

References:

[1] C. Zhang, Y. Xu, M. Zhou, L. Liang, H. Dong, M. Wu, Y. Yang and Y. Lei, *Advanced Functional Materials* **2017**, *27*, 1604307.

[2] a) G. Kresse and J. Furthmüller, *Physical Review B* **1996**, *54*, 11169-11186; b) G. Kresse and J. Furthmüller, *Computational Materials Science* **1996**, *6*, 15-50.

[3] P. E. Blöchl, *Physical Review B* **1994**, *50*, 17953-17979.

[4] J. P. Perdew, K. Burke and M. Ernzerhof, *Physical Review Letters* **1996**, *77*, 3865-3868.